

## Effect of N<sub>2</sub> flow rates on the structure and hardness of nanocrystalline CrZrN thin films prepared by reactive DC magnetron co-sputtering

Siriwat Alaksanasuwan<sup>1</sup> and Nirun Witit-anun<sup>2\*</sup>

### Abstract

This work successfully investigated the effect of N<sub>2</sub> gas flow rates on the structure and hardness of chromium zirconium nitride (CrZrN) thin films. The CrZrN films were deposited on silicon wafers using a reactive DC unbalance-magnetron co-sputtering process with N<sub>2</sub> flow rates ranging from 4 to 10 sccm. The crystal structure was investigated using grazing-incidence X-ray diffraction (GI-XRD). Field-emission scanning electron microscopy (FE-SEM) was used to examine the included material's microstructure, surface morphology, and thickness. The elemental composition was determined using energy dispersive spectroscopy (EDS). The hardness was measured using the nanoindentation method in depth-controlled mode. The results reveal that the as-deposited films were formed as a nanocrystalline (Cr,Zr)N solid solution with small crystal sizes less than 10 nm. Increasing the N<sub>2</sub> flow rate altered the preferred orientation growth behavior by decreasing the 2 $\theta$ -values and increasing the lattice constants. The thickness decreased from 569 nm to 410 nm as the N<sub>2</sub> flow rate increased, due to target poisoning. The elemental composition of the as-deposited films was affected by changes in the N<sub>2</sub> flow rates. The N content increased with higher N<sub>2</sub> flow rates, while the Cr and Zr contents decreased. The surface morphology of the films changed as the N<sub>2</sub> flow rate increased, due to the reduction in ion-bombardment energy, leading to a decrease in substrate temperature. The as-deposited films consisted of tiny grains, which grew larger with increasing N<sub>2</sub> flow rates. Cross-sectional analysis showed that the films exhibited a compact columnar structure. The hardness of CrZrN films in this study ranged from 13.1 to 13.8 GPa at various N<sub>2</sub> flow rates.

**Keywords:** CrZrN, hard coating, magnetron sputtering, N<sub>2</sub> flow rates, thin films

---

<sup>1</sup> Faculty of Science and Technology, Phranakhon Si Ayutthaya Rajabhat University

<sup>2</sup> Faculty of Science, Burapha University

\* Corresponding author. E-mail: nirun@buu.ac.th

## Introduction

Surface engineering is an important technique generally used to improve the required performance of industrial materials, such as tribological properties and thermal stability. Principally, high-speed cutting tools must withstand aggressive environments, including high temperatures, friction, and corrosion between materials. To address these challenges, the application of thin hard coatings that protect tools against wear is state of the art (Bobzin et al., 2021; Krelling et al., 2017). Transition-metal nitride coatings, such as binary nitrides (e.g., TiN, CrN, VN, etc.), are good candidates for use as protective coatings to extend the lifetime of tools (Luo et al., 2023). Among them, CrN films are widely used in manufacturing items due to their high hardness, low friction coefficient, and oxidation resistance at high temperature (around 800°C) (Qi et al., 2013; Wu et al., 2016). These characteristics make CrN ceramic coating an excellent candidate for protective coating in cutting tools, forming tools, dies, and wear protection, serving as a replacement for chromium electroplating (Subramanian et al., 2013).

Later, it was found that the mechanical and thermal properties of CrN films could be improved by alloying Zr atoms into CrN to form a ternary nitride of CrZrN films. Thus, CrZrN films are ceramic hard coatings with several advantageous characteristics, such as better mechanical properties and very low surface roughness (Kim et al., 2013). Additionally, the structure and mechanical properties of CrZrN films strongly depend on the concentration of Zr. Witit-anun & Buranawong (2023) showed that varying Zr content in CrZrN films deposited by reactive magnetron sputtering resulted in changes in surface roughness and grain refinement. Khamseh & Araghi (2016) reported that the denser, compact structure and lower surface roughness of CrZrN films prepared by magnetron sputtering were observed with increasing Zr content. The hardness and wear resistance were also much higher than those of CrN films. Feng et al., (2018) studied the structure, morphology, and mechanical properties of CrZrN films deposited with different Zr contents. They showed that the hardness and modulus increased, while the wear rate decreased with increasing Zr content.

It is clear that many researchers have focused on the Zr content in CrZrN films. However, few studies have addressed changes in the microstructure and mechanical properties of CrZrN films with varying  $N_2$  flow rates. It is well known that the microstructure and many properties of sputtered films depend on several deposition parameters, such as  $N_2$  flow rates, sputtering power, pressure, substrate temperature, and voltage bias. Therefore, N content may also be an important parameter for controlling the performance of ternary nitride films. Tsai et al., (2011) reported that the deposition rate of the (TiVCr)N films deposited by RF magnetron sputtering decreased with an increasing  $N_2$ -to-total ( $N_2 + Ar$ ) flow ratio ( $R_N$ ). They demonstrated that increasing  $R_N$  altered the structure and hardness of (TiVCr)N films. The preferred orientation changed from (111) to (200). The microstructure transformed from a columnar structure with void boundaries and a rough-faceted surface to a dense structure. The hardness increased with increasing of  $R_N$ .

As mentioned previously, this work aims to investigate the effect of  $N_2$  flow rates on the microstructure and hardness of nanocrystalline CrZrN films prepared by reactive magnetron co-sputtering. The microstructure of the as-deposited films-including crystal structure, surface morphology, and elemental composition was

studied. Additionally, the hardness of the films was measured. These data were used to describe an advanced method for understanding the film's structure. Moreover, this work may contribute to achieving hard coating applications for industrial facilities.

### Methodology

The CrZrN films were prepared using a homemade vacuum coater with a reactive DC unbalanced magnetron sputtering system. The vacuum chamber is a cylindrical stainless-steel coating chamber, measuring 31 cm in diameter and 37 cm in height. The sputtering targets, Cr and Zr, have a diameter of 5.40 cm and a thickness of 0.30 cm and are held on a water-cooled magnetron cathode. The substrates were silicon wafers, located at a distance of 13 cm from the targets. The processing gas consisted of Ar (sputtering gas) and N<sub>2</sub> (reactive gas), which were controlled by mass flow controllers (MKS type 247D). Before introducing of the processing gases, ambient air in the chamber was evacuated to a base pressure of  $5.0 \times 10^{-5}$  mbar by a diffusion pump backed with a rotary pump. Prior to deposition, the pre-sputtering process was initiated using Ar<sup>+</sup> ions bombardment to eliminate the impurities from target surface, with a shutter shielding for approximately 5 min. The Ar flow rate was always controlled as a constant at 10 sccm. Whereas the N<sub>2</sub> flow rate varied from 4 to 10 sccm in 2 sccm increments. The working pressure was maintained as  $5.0 \times 10^{-3}$  mbar. The sputtering power of Cr and Zr were maintained as 400 W and 350 W, respectively. These parameters were controlled throughout as a deposition time of 60 min. The details of the deposition parameters are shown in (Table 1).

**Table 1** Thin films deposition conditions.

| parameters                    | details                     |
|-------------------------------|-----------------------------|
| sputtering target             | Cr (99.95%) and Zr (99.95%) |
| temperature                   | room temperature            |
| target to substrate distance  | 130 mm                      |
| base pressure                 | $5.0 \times 10^{-5}$ mbar   |
| working pressure              | $5.0 \times 10^{-3}$ mbar   |
| sputtering power of Cr target | 400 W                       |
| sputtering power of Zr target | 350 W                       |
| Ar flow rate                  | 10 sccm                     |
| N <sub>2</sub> flow rates     | 4, 6, 8, 10 sccm            |
| deposition time               | 60 min                      |

The as-deposited CrZrN films were characterized by several techniques to study their microstructure and hardness. Crystal structures were analyzed by grazing-incidence X-ray diffraction (GI-XRD: Bruker D8) using a Cu-K $\alpha$  radiation ( $\lambda=0.154$  nm). The XRD patterns were studied in a continuous mode with a scanning speed of 2°/min and a grazing incidence angle of 3°. Phases were identified by an interplanar spacing equation and

compared with the joint committee on powder diffraction standard (JCPD) files. Crystal sizes were calculated from the FWHM of the XRD pattern by Scherrer's equation. The microstructure, surface morphology, and cross-sectional analysis were investigated by field emission scanning electron microscope (FE-SEM: Hitachi S-4700). The elemental composition in terms of atomic percentages was measured by energy dispersive X-ray spectroscopy (EDS: EDAX) which was equipped with a scanning electron microscope (SEM: LEO 1450VP). Lastly, the hardness of the as-deposited films was measured by nano-indenter (BRUKER: Hysitron TI Premier) as a Berkovich indent probe under depth-controlled mode. The indentation depth was controlled as less than one-tenth of the film thickness at a maximum load of 1.50 mN.

### Results and Discussion

The crystal structures of the as-deposited CrZrN films prepared on Si wafers at different  $N_2$  gas flow rates in the range of 4-10 sccm, were analyzed by the XRD technique. The XRD patterns are shown in (Figure 1). The diffraction angles ( $2\theta$ -values) of CrN (JCPDS No. 77-0047) and ZrN (JCPDS films No. 78-1420) at (111) and (200) were shown by dash lines for comparison purposes. From the results of the XRD pattern, it is clearly seen that the films showed crystalline phases of FCC-type structure. Foremost, the  $2\theta$ -values were located between the standard of CrN and ZrN. These results confirmed that the as-deposited films formed a (Cr,Zr)N solid-solution. Furthermore, it was found that the  $N_2$  flow rates strongly influenced the crystal structure of the films. As the  $N_2$  flow rates increased, the  $2\theta$ -values were continuously decreased from  $35.9^\circ$  to  $35.1^\circ$  and  $41.8^\circ$  to  $41.40^\circ$  for (111) and (200), respectively (Figure 2). It implied that the shift to the lower angle of  $2\theta$ -values occurred by amount of larger Zr atoms increased (atomic radius of Zr is 0.161 nm), which were replaced for the smaller Cr atoms (atomic radius of Cr is 0.136 nm) in the crystal structure (Kim et al., 2005). Additionally, the preferred orientation of (111) was decreased with increasing of  $N_2$  flow rates. Whereas, the preferred orientation of polycrystalline with high intensity of (200) is shown as the  $N_2$  flow rate increased to 4 sccm. After that, it was found that the films also showed the polycrystalline with lower crystallinity of (200), as the  $N_2$  flow rate increased from 6 to 10 sccm.

The results for crystal sizes and lattice constants are shown in (Table 2). In fact, the crystal sizes and the lattice constants depended on the  $N_2$  gas flow rate. The crystal size of the preferred orientations of (111) and (200) ranged from 7.60-8.50 nm. The lattice constants of (111) and (200) increased with increasing of  $N_2$  flow rate from 4.326 Å to 4.428 Å and 4.317 Å to 4.362 Å for (111) and (200), respectively (Figure 2). The increase in lattice constant possibly will be the results of the substitution of Cr with Zr in the CrN lattice (Kim et al., 2005). Moreover, the lattice constant also varied between the standard of CrN (4.148 Å) and ZrN (4.585 Å), which can also support the results from the XRD.

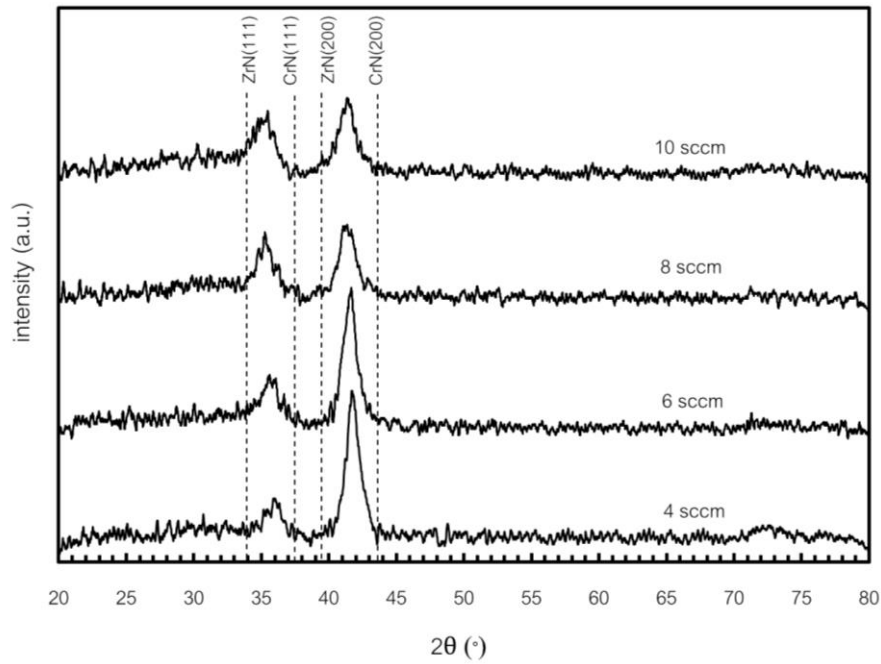


Figure 1 XRD patterns of CrZrN thin films deposited at various  $N_2$  flow rates.

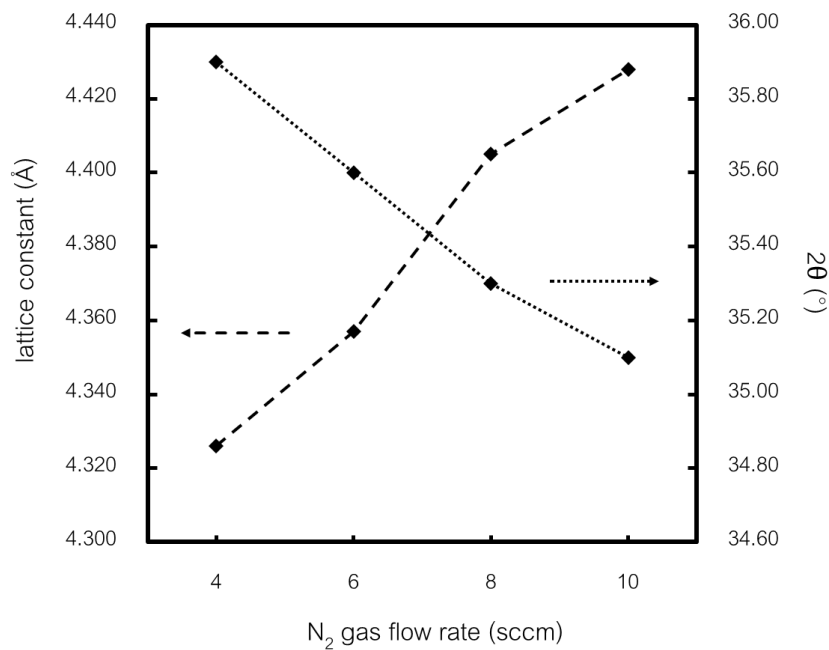


Figure 2 The  $2\theta$ -values and the lattice constants of CrZrN thin films as a function of  $N_2$  flow rates.

These results indicate that the  $N_2$  gas flow rate in the sputtering gas mixture significantly affected the orientation growth behavior. It was found that Zr atoms were incorporated into the CrN structure, due to the diffraction peaks corresponding to the CrN and ZrN phases were not found. Therefore, the sputtered Zr atoms were dissolved into CrN structure (by substitutional replacement of Zr atoms for Cr sites). Where, the larger atomic radius of Zr (0.145 nm) substituted the lattices of a smaller atomic radius of Cr (0.118 nm). This result suggests

that the as-deposited thin films were completely formed as a solid-solution (Cr,Zr)N structure. This result is in agreement with other reports in a part of the literature review.

**Table 2**  $2\theta$ -values, crystal sizes and lattice constants of CrZrN thin films at various  $N_2$  flow rates.

| $N_2$ flow rates<br>(sccm) | $2\theta$ -values (degree) |       | crystal size (nm) |       | lattice constants (Å) |       |
|----------------------------|----------------------------|-------|-------------------|-------|-----------------------|-------|
|                            | (111)                      | (200) | (111)             | (200) | (111)                 | (200) |
| 4                          | 35.90                      | 41.80 | 7.90              | 8.50  | 4.326                 | 4.317 |
| 6                          | 35.60                      | 41.60 | 7.90              | 8.50  | 4.357                 | 4.337 |
| 8                          | 35.30                      | 41.40 | 7.60              | 8.50  | 4.405                 | 4.357 |
| 10                         | 35.10                      | 41.40 | 8.00              | 8.00  | 4.428                 | 4.362 |

The microstructure of the CrZrN thin films deposited at different  $N_2$  flow rates is shown in (Figure 3). The large grains were shown as the low  $N_2$  flow rate of 4 sccm. As the  $N_2$  flow rate increased, the denser and smaller grains with smooth surfaces were shown. The surface morphologies of films are changed due to the lower of ion-bombarding and substrate temperature as the  $N_2$  flow rate increased. It is related to the energy accompanied as an increasing Zr/Cr flux (Chantharangsi et al., 2015).

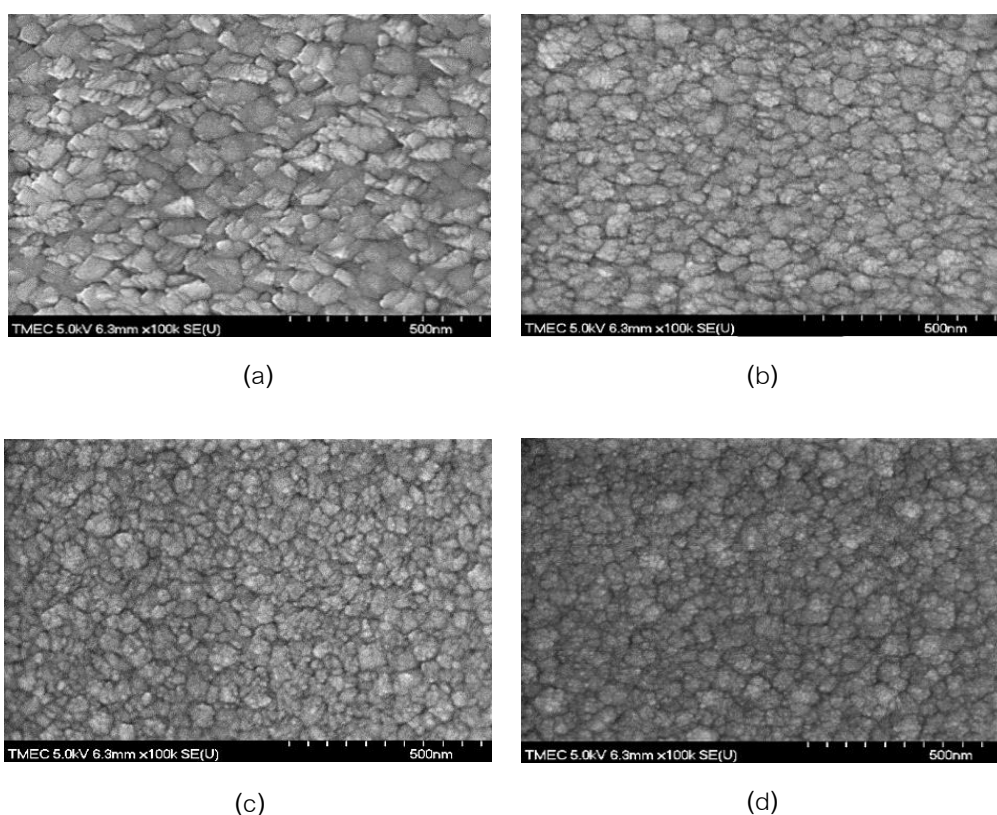


**Figure 3** The microstructure of the CrZrN thin films at various  $N_2$  flow rates: (a) 4 sccm, (b) 6 sccm, (c) 8 sccm, and (d) 10 sccm.

The cross-section analysis was clearly identified that the thickness was changed with varying of  $N_2$  flow rates. The thickness was measured by the cross-section analysis from the FE-SEM micrograph as also shown in (Figure 4). The film's thickness was decreased from 569 to 410 nm with an increasing of  $N_2$  flow rate. Similarly, the deposition rate was reduced from 9.50 to 6.80 nm/min as  $N_2$  flow rate increased. It was visibly indicated that the increasing of  $N_2$  flow rates is cause of the reducing of sputtering yield by target poisoning. On the other hand, since the total gas mixture flow rate is a constant, an increasing of  $N_2$  flow rate occur as a decreasing of Ar concentration. Therefore, the sputtering yield was reduced due to the lower momentum transfer of  $N_2$  compared to Ar (Zhang et al., 2000). Moreover, the microstructure of the CrZrN films deposited at low  $N_2$  flow rates also shows a compact columnar structure, corresponding to zone 2 of the Thornton's structure zone model (SZM). After that, the dense structure was shown as deposited at high  $N_2$  flow rates. As the Zr content increased, ion bombarding with higher energy resulted in a dense microstructure through the grain refinement (Chantharangsi et al., 2012).

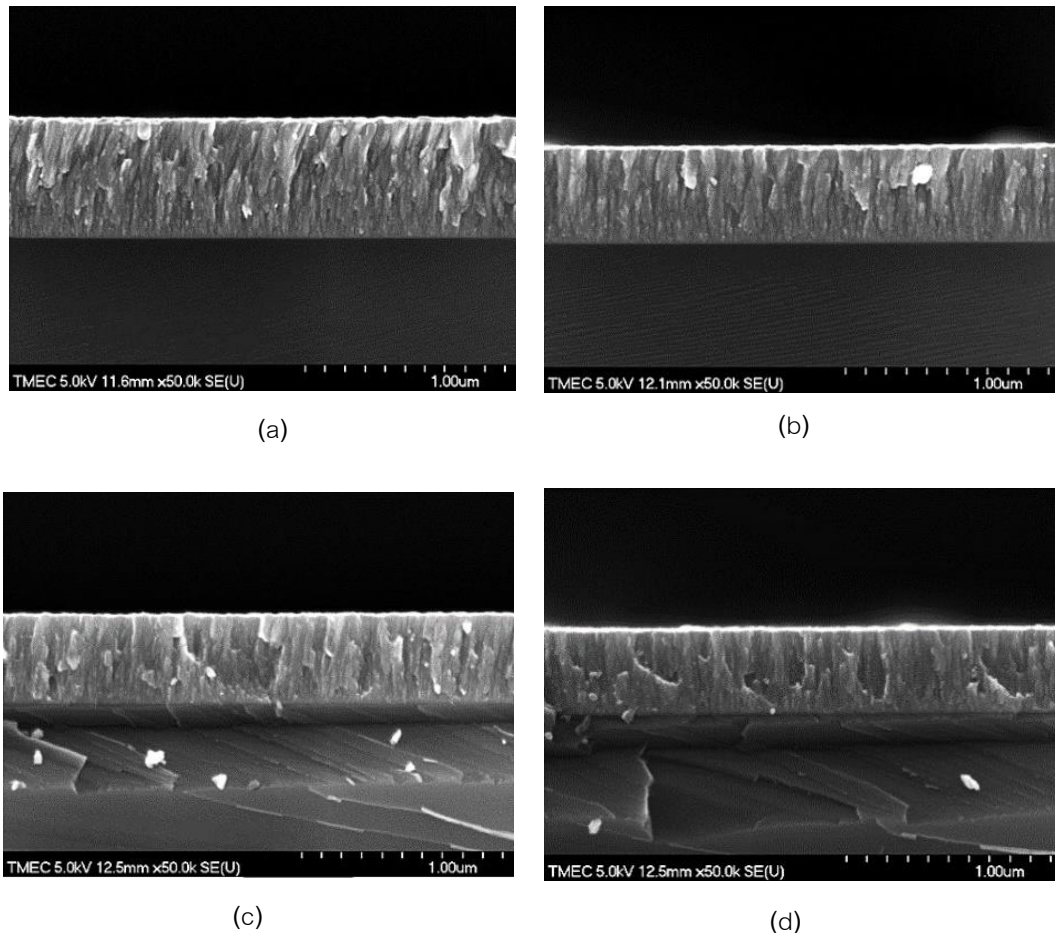


**Figure 4** The cross-sectional analysis of the CrZrN thin films at various  $N_2$  flow rates: (a) 4 sccm, (b) 6 sccm, (c) 8 sccm, and (d) 10 sccm.



The elemental composition measured by energy dispersive spectroscopy (EDS) of the CrZrN thin films at various  $N_2$  flow rates is shown in (Figure 5). It reveals that the N content continuously increased with increasing  $N_2$  flow rates. Whereas the concentrations of Cr and Zr were slightly decreased. (Table 3) shows that the N content increased from 51.30 to 64.80% following on  $N_2$  flow rates from 4 to 10 sccm. Additionally, the stoichiometric (Cr,Zr) N film were obtained by used as  $N_2$  flow rates of 4 sccm. In this case, it was found that a ratio of metallic content (Cr+Zr) and N content was closed to 1:1.

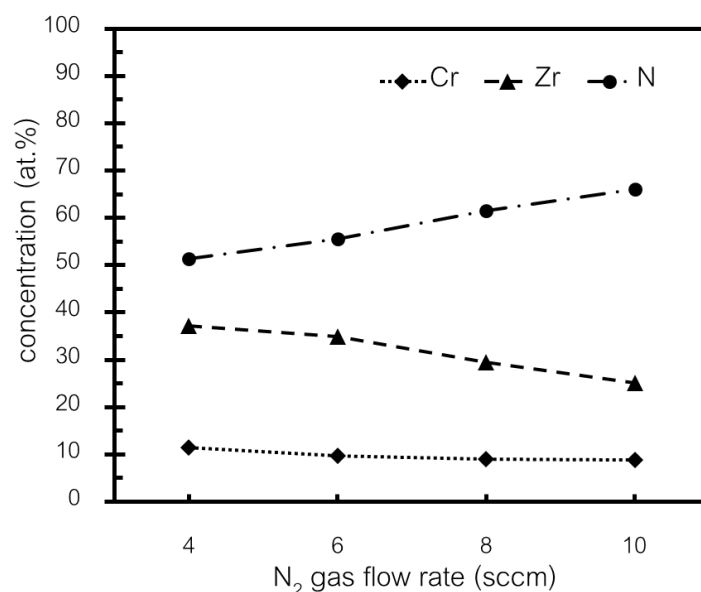


Figure 5 Concentration of elements in CrZrN films as a function of  $N_2$  flow rates.

The hardness of CrZrN films was calculated from the load-unload displacement curve. It is commonly accepted that the ratio of the indentation depth is around a 1/10 of the total thickness by the nano-indentation technique. In this study, the as-deposited films showed a slight decrease of hardness as the  $N_2$  flow rate increased, ranging from 13.80 to 13.10 GPa (Table 3). It can be attributed mainly to the high density of the voids between the columns, due to the evolutionary overgrowth mechanism (Tsai et al., 2011).

Table 3 Some properties of CrZrN thin films at various  $N_2$  flow rates.

| $N_2$ flow rate<br>(sccm) | thickness<br>(nm) | deposition rate<br>(nm/min) | Cr<br>(at.%) | Zr<br>(at.%) | N<br>(at.%) | hardness<br>(GPa) |
|---------------------------|-------------------|-----------------------------|--------------|--------------|-------------|-------------------|
| 4                         | 569               | 9.50                        | 11.50        | 37.20        | 51.30       | 13.80             |
| 6                         | 463               | 7.70                        | 9.60         | 34.80        | 55.60       | 13.80             |
| 8                         | 456               | 7.60                        | 8.90         | 29.60        | 61.50       | 13.20             |
| 10                        | 410               | 6.80                        | 8.70         | 26.50        | 64.80       | 13.10             |



### Conclusion

The CrZrN thin films were successfully prepared by using DC reactive magnetron co-sputtering at different N<sub>2</sub> flow rates of 4, 6, 8, and 10 sccm. The crystal structures, microstructures, surface morphologies, elemental compositions, and hardness were strongly dependent on the N<sub>2</sub> flow rates. The results showed that the as-deposited films had a B1-NaCl structure of (Cr,Zr)N with preferred orientation of (111) and (200). The variation of N<sub>2</sub> flow rate influenced the preferred orientation growth behavior. The 2 $\theta$ -values were decreased from 35.9° to 35.1° and 41.8° to 41.4° for (111) and (200) with an increasing N<sub>2</sub> flow rate. The lattice constants were increased from 4.326 Å to 4.428 Å for (111) and 4.317 Å to 4.362 Å for (200) with increasing of the N<sub>2</sub> flow rate. The crystal sizes were very small, in the range of 7.6 to 8.5 nm. The thickness reduced from 569 nm to 410 nm, with an opposite increase in the N<sub>2</sub> flow rate due to target poisoning. The N content increased, while the Cr content and Zr content were decreased, with increasing of N<sub>2</sub> flow rate. The surface morphologies of films changed from the large grain to small grain and denser as the N<sub>2</sub> flow rate increases. The cross-sectional analysis of films showed the compact columnar. The hardness of films (obtained by the nano-indentation technique) were slightly decreased from about 13.8 to 13.1 GPa, due to the evolutionary overgrowth mechanism.

### References

- Bobzin, K., Brogelmann, T., Maier, H. J., Heidenblut, T., Kahra, C., & Carlet, M. (2021). Influence of residual stresses in hard tool coatings on the cutting performance. *Journal of Manufacturing Processes*, 69, 340-350. <https://doi.org/10.1016/j.jmapro.2021.08.011>
- Chantharangsi, C., Denchitcharoen, S., Chaiyakun, S., & Limsuwan, P. (2012). Structure and surface morphology of Cr-Zr-N thin films deposited by reactive DC magnetron sputtering. *Procedia Engineering*, 32, 868-874. <https://doi.org/10.1016/j.proeng.2012.02.025>
- Chantharangsi, C., Denchitcharoen, S., Chaiyakun, S., & Limsuwan, P. (2015). Structures, morphologies, and chemical states of sputter-deposited CrZrN thin films with various Zr contents. *Thin Solid Films*, 589, 613-619. <https://doi.org/10.1016/j.tsf.2015.06.045>
- Feng, X. G., Zhang, K. F., Zheng, Y. G., Zhou, H., & Wan, Z. H. (2018). Structure, morphologies and mechanical properties study of Cr-Zr-N films. *Nuclear Instruments and Methods in Physics Research Section B: Beam Interactions with Materials and Atoms*, 436, 112-118. <https://doi.org/10.1016/j.nimb.2018.09.009>
- Khamseh, S., & Araghi, A. (2016). A study of the oxidation behavior of CrN and CrZrN ceramic thin films prepared in a magnetron sputtering system. *Ceramics International*, 42, 9988-9994. <https://doi.org/10.1016/j.ceramint.2016.03.101>
- Kim, G. S., Kim, B. S., Lee, S. Y., & Hahn, J. H. (2005). Structure and mechanical properties of Cr-Zr-N films synthesized by closed field unbalanced magnetron sputtering with vertical magnetron sources. *Surface and Coating Technology*, 200, 1669-1675. <https://doi.org/10.1016/j.surfcoat.2005.08.101>
- Kim, D. J., Kim, S. M., La, J. H., Lee, S. Y., Hong, Y. S., & Lee, M. H. (2013). Synthesis and characterization of CrZrAlN films using unbalanced magnetron sputtering with segment targets. *Metal and Material International*, 19(6), 1295-1299. <https://link.springer.com/article/10.1007/s12540-013-6023-x>

- Krelling, A. P., da Costa, C. E., Milan, J. C. G., & Almeida, E. A. S. (2017). Micro-abrasive wear mechanisms of borided AISI 1020 steel. *Tribology International*, 111, 234-242. <https://doi.org/10.1016/j.triboint.2017.03.017>
- Luo, Q., Lu, C. C., Liu, L. R., & Zhu, M. Y. (2023). A review on the synthesis of transition metal nitride nanostructures and their energy related applications. *Green Energy & Environment*, 8, 406-437. <https://doi.org/10.1016/j.gee.2022.07.002>
- Qi, Z. B., Liu, B., Wu, Z. T. Zhu, F. P., Wang, Z. C., & Wu, C. H. (2013). A comparative study of the oxidation behavior of Cr<sub>2</sub>N and CrN coatings. *Thin Solid Films*, 544, 515-520. <https://doi.org/10.1016/j.tsf.2013.01.031>
- Subramanian, B., Prabakaran, K., Thampi, V. V. A., & Jayachandran, M. (2013). Electrochemical noise analysis on sputtered chromium nitride coated D9 steels. *International Journal of Electrochemical Science*, 8, 12015-12027. [https://doi.org/10.1016/S1452-3981\(23\)13239-1](https://doi.org/10.1016/S1452-3981(23)13239-1)
- Tsai, D. C., Huang, Y. L., Lin, S. R., Jung, D. R., Chang, S. Y., & Shieu, F. S. (2011). Structure and mechanical properties of (TiVCr)N coatings prepared by energetic bombardment sputtering with different nitrogen flow ratios. *Journal of Alloys and Compounds*, 509, 3141-3147. <https://doi.org/10.1016/j.jallcom.2010.12.026>
- Witit-anun, N., & Buranawong, A. (2023). Effect of Zr content on the structure and hardness of CrZrN thin films prepared by reactive DC magnetron co-sputtering method. *RMUTSB Academic Journal*, 11(2), 172-185. <https://li01.tci-thaijo.org/index.php/rmutsb-sci/article/view/258773/177320> (in Thai)
- Wu, Z. T., Qi, Z. B., Zhang, D. F., Wei, B. B., & Wang, Z. C. (2016). Evaluating the influence of adding Nb on microstructure, hardness and oxidation resistance of CrN coating. *Surface and Coatings Technology*, 289, 45-51. <https://doi.org/10.1016/j.surfcoat.2016.01.047>
- Zhang, D. H., Yang, T. L., Ma, J., Wang, Q. P., Gao, R. W., & Ma, H. L. (2000). Preparation of transparent conducting ZnO:Al films on polymer substrates by r. f. magnetron sputtering. *Applied Surface Science*, 158, 43-48. [https://doi.org/10.1016/S0169-4332\(99\)00591-7](https://doi.org/10.1016/S0169-4332(99)00591-7)